

Population size effects in evolutionary dynamics on neutral networks and toy landscapes

Sumedha¹, Olivier C. Martin^{1,2}, and Luca Peliti³

¹ Université Paris-Sud, UMR8626, LPTMS, Orsay, F-91405; CNRS, Orsay, F-91405, France

² UMR de Génétique Végétale du Moulon, INRA-UPS-CNRS-INA PG, F-91190 Gif-sur-Yvette, France

³ Dipartimento di Scienze Fisiche, Sezione INFN and Unità CNISM, Università di Napoli “Federico II”, Complesso Universitario di Monte S. Angelo, I-80126 Napoli, Italy

E-mail: sumedha.sumedha@gmail.com, olivier.martin@u-psud.fr, Luca.Peliti@na.infn.it

Abstract. We study the dynamics of a population subject to selective pressures, evolving either on RNA neutral networks or in toy fitness landscapes. We discuss the spread and the neutrality of the population in the steady state. Different limits arise depending on whether selection or random drift are dominant. In the presence of strong drift we show that observables depend mainly on $M\mu$, M being the population size and μ the mutation rate, while corrections to this scaling go as $1/M$: such corrections can be quite large in the presence of selection if there are barriers in the fitness landscape. Also we find that the convergence to the large $M\mu$ limit is linear in $1/M\mu$. Finally we introduce a protocol that minimizes drift; then observables scale like $1/M$ rather than $1/(M\mu)$, allowing one to determine the large M limit faster when μ is small; furthermore the genotypic diversity increases from $O(\ln M)$ to $O(M)$.

PACS numbers: 87.23.-n (Ecology and evolution), 87.15.Aa (Theory and modeling; computer simulation), 89.75.Hc (Networks and genealogical trees)

Submitted to: *JSTAT*

Keywords: evolutionary dynamics, neutral networks, drift, selection

1. Introduction

In evolutionary biology, populations are subject to a number of forces that shape their genetic composition [1]. Amongst these, mutations, selection and drift play a central role. Drift becomes dominant for small populations, while for large populations one reaches a steady state where mutations balance effects of selection. The landscape paradigm [2, 3] provides a relation between genotype/phenotype and fitness, allowing for quantitative studies of evolving populations, while at the same time giving a qualitative picture. This has been particularly developed in the context of quasispecies theory [4, 5, 6] and of evolution on networks [7, 8]; in a different framework these problems have been analyzed within evolutionary game theory [9, 10, 11, 12] although, in that case, usually there is no drift in the usual sense and the number of genotypes is low.

Let us consider a population of M individuals evolving in a static fitness landscape. We can define its steady-state distribution from the average number of individuals with a given genotype, averaged over a long stretch of time. One can also consider how the population is spread out in genotype space. If all genotypes have the same fitness (flat landscape), the steady state distribution is independent of M while the spread of the population depends mainly on the product $M\mu$ where μ is the mutation rate [13]. In the limit of an infinite population (μ fixed), the generation-to-generation fluctuations vanish and the instantaneous population distribution coincides with the steady-state one. This is the quasispecies limit, where the steady-state distribution is given by the leading eigenvector of the evolution operator [14]. When the population is finite, no general analytic solution for the steady-state distribution is known. If the population size is much greater than the number of genotypes, then the so-called diffusion approximation [15] can be used. However, in most realistic cases, the number of possible genotypes is much greater than the population size. We are interested in understanding how mutation, selection and drift affect different properties of the steady state in such systems.

To unravel the different effects, we consider different evolutionary dynamics, in which some of these processes may be present or not. Most of our study is conducted in the framework of RNA neutral networks [16, 8], the archetypes of genotype to phenotype mappings, but we also consider toy fitness landscapes. After specifying our systems and population dynamics in sections 2 to 4, we examine the dependence on the mutation rate μ and on M of the different processes driving the dynamics. We begin with the case of neutral evolution in section 5, turning on and off the drift. In section 6 we allow for selection in the usual way that leads to significant drift. As a general rule, drift in these situations leads to $M\mu$ scaling, as shown previously in the absence of selection [13]. Then in section 7 we introduce a particular dynamics with selection but *low drift*. There the $M\mu$ scaling is replaced by a smooth large M limit even when $\mu \rightarrow 0$; furthermore the genotypic diversity becomes proportional to M rather than being nearly constant. The corrections to these scalings generically go as $O(1/M)$, with large effects when there

are barriers in the landscape, as we exhibit in section 8. Section 9 is devoted to some final considerations.

2. RNA neutral networks as fitness landscapes

In studies of genotype to phenotype mappings, one often focuses on biological molecules because the corresponding mapping is relatively well defined. The genotype is simply the sequence of the bio-molecule, while the phenotype is its shape, as specified for instance by the minimum free-energy structure it folds into. Using either protein or secondary RNA structures, it has been found [8, 16, 17, 18] that neutral genotypes (genotypes that have a given phenotype) which are connected via single mutational steps form extended networks that permeate large regions of genotype space. These are known as “neutral networks”. Via the neutral network, a population can move in genotype space without crossing unfavorable low-fitness regions, in contrast to what happens in many rugged fitness landscapes [2, 19, 20, 21]. However, because of the huge dimensionality of our genotype space, large neutral (or nearly neutral) networks can be argued to be inevitable [3].

Here we shall work with an RNA neutral network, i.e., all RNA sequences which fold into a given target RNA secondary structure. The genotype of an RNA molecule is given by its base sequence: there are four bases, A,C,G, and U, and thus 4^L genotypes for molecules of L bases. The molecule’s phenotype is given by its *secondary* structure, i.e., by which bases are paired with which as occur in its folded form. To every genotype one associates just one phenotype (the secondary structure of minimum free energy) while in general there will be many genotypes compatible with a given phenotype. This many-to-one genotype to phenotype mapping has been widely studied [8, 14, 16, 18, 22, 23, 24]. Standard computational tools are available on the web to fold given sequences; see for instance the *fold* subroutine from the Vienna package [25] which we used for all of this work’s computations. Two sequences are nearest neighbors (connected on the neutral network) if and only if they differ by a single nucleotide substitution. In general, RNA neutral networks are heterogenous graphs, so that for instance the local connectivity varies quite a lot from site to site.

The secondary structure (phenotype) chosen in this study is the one used by van Nimwegen et al. [14, 21]: it has 18 nucleotides with six base pairs and is depicted in figure 1. By single-nucleotide substitutions, purine-pyrimidine base pairs (G–C, G–U, A–U) can mutate into each other, but not into pyrimidine-purine (C–G, U–G, U–A) base pairs. Hence we considered only the purine-pyrimidine base pairs. Given the base pairing rules for this system, the number of a priori “compatible” sequences for such a structure is $4^6 \times 3^6 = 2985884$. At 30°C, 37963 of these fold into the target structure; this number depends a bit on the choice of temperature since the *fold* algorithm computes free energies. We find these genotypes to be organized into *three* neutral networks (connected components), of sizes 489, 5784 and 31484 respectively. This will allow us to investigate the effect of neutral network size on our observables.

4. The model

Many processes affect the genetic makeup of natural populations. In this work, we focus on the effects of mutation, selection and drift. We wish to turn on and off selection or even drift while considering the effects of the population size M or of the mutation rate μ . Thus the details of the evolutionary process we consider are tailored to emphasize one or another of these aspects at a time.

We consider a population evolving with nonoverlapping generations; the population size is kept at a fixed value in the standard way. Other choices could have been made, but as in most studies, the detailed procedures used in the evolutionary dynamics is not expected to be very important.

Given the M individuals at the current generation, we must produce M viable offspring to form the next generation. Each offspring is produced from a parent and given a chance to mutate: with probability $1 - \mu$, no mutation is applied, and with probability μ one base at random is changed. Then *selection* is applied: the child is kept if and only if it is viable. More generally, on an arbitrary fitness landscape, we let it survive stochastically according to its fitness. Of course if there is no selection, the offspring is always kept. The process of producing offspring is repeated until the new generation has size M . *Drift* comes in via the way the parents are chosen to produce candidate offspring. In the standard method, the parents are chosen randomly *with replacement*: clearly this allows for drift as by bad luck some parents will not produce any offspring. In the presence of selection, drift cannot be turned off completely but it can be significantly lowered.

Indeed, let us consider the following process. First, each individual of the population produces one offspring which mutates with probability μ : if a mutation is lethal, the corresponding offspring is killed. In this step there is no replacement and the resulting offspring population size will generally be smaller than M . Second, one chooses individuals randomly from this offspring population and replicates them. This is done until the population size reaches M again. Note that when μ is small, the new generation will be nearly identical to the previous one, even for small M , so there is very little drift. Because of selection, a small amount of drift does occur, but its intensity is proportional to μ .

In all our runs, we initialize arbitrarily the population and let it evolve for a large number of generations until initial conditions are forgotten: this is the steady state limit. All the data presented in this work are time averages taken from this regime. We are now ready to see how M , μ , drift and selection affect the spread, neutrality and the genotypic diversity of the steady state population.

5. Dynamics without selection

In this section, we consider a population evolving without being subject to selection. We investigate the effects of allowing or not drift, first on regular networks and then on

heterogeneous ones.

5.1. Homogeneous networks

Consider the space of sequences of length L ; if we take these to all be viable, then we get a homogeneous network in which all 1-mutant neighbors of each genotype belong to the network. Derrida and Peliti [13] studied the evolution of a population on such a flat fitness landscape. Using the fact that there is no selection, it is easy to show that the steady state distribution is *uniform*. Thus the population neutrality is trivial, being given by the degree of the network, i.e., $3L$, for all population sizes. In contrast to this simple result, the distribution of Hamming distances between genotypes in the population is generally non-trivial. Depending on the nature of the dynamics, we have the following behaviors:

- (a) Drift off — The offspring are produced from parents *without replacement*: since each individual has exactly one offspring, each lineage acts like an independent random walk. Thus the Hamming distances between the genotypes in the population are completely random: the mean of h lies at $3L/4$ (at each position along the sequence, one has a $3/4$ chance of having different bases when comparing two random sequences) and its variance is equal to $3L/16$.
- (b) Drift on — Here the offspring are produced from parents *with replacement*: the number of offspring of an individual is variable, leading to tree genealogies. This situation incorporating drift was studied by Derrida and Peliti [13] and leads to a non-trivial $P(h)$ which depends on M and μ . At any given generation, the individuals have mutual distances that reflect the fact that they descend from a common ancestor, giving rise to a clustering of the population that fluctuates from one generation to the next. For our purposes here, we focus on the result [13] that the relevant parameter when M is large is $M\mu$: in particular, $P(h)$ depends only on the product $M\mu$ at large M , a property that we call $M\mu$ scaling.

5.2. RNA neutral networks

We now consider a population evolving on an RNA neutral network, defined as the subspace of sequences which fold (at 30°C) into the target secondary structure shown in figure 1. RNA neutral networks are generally heterogeneous. Evolutionary dynamics without selection can be implemented by simply “forbidding” attempts to apply lethal mutations. There are two natural ways to do this, referred to as blind and myopic ant dynamics [27]. In myopic ant dynamics, also called adaptive random walks [19, 20, 28], an offspring that mutates is forced to choose a single point mutation that is non-lethal (all non-lethal choices are equiprobable). In blind ant dynamics (also called gradient random walks), a point mutation is chosen at random (lethal or not): if it is non-lethal, it is accepted, while if it is lethal, it is refused and the offspring is taken to be *non-mutant*. Both the blind and myopic dynamics can be implemented with or without drift,

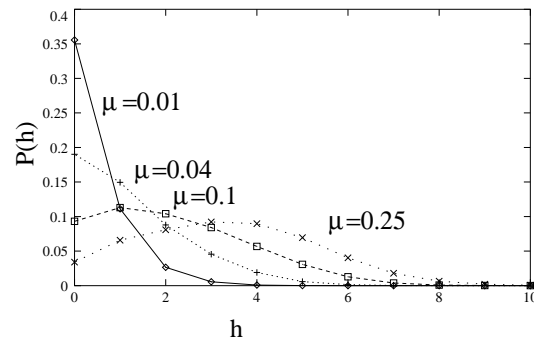


Figure 2. Distribution of Hamming distances h for different values of μ for the myopic ant dynamics in the presence of drift. The population size is $M = 20$.

according to the method sketched in section 4. Although these dynamical processes may appear to be somewhat artificial, they do provide solvable cases. Furthermore, van Nimwegen et al. [14] have shown that in the limit of small $M\mu$, the standard evolutionary dynamics converges to the blind ant dynamics.

Consider first the case without drift, in which the sampling of the parents takes place *without replacement*. Then each lineage performs an independent random walk on the whole neutral network. As shown by van Nimwegen et al. [14], the steady-state distribution for blind ants is uniform on the neutral network, while for myopic ants the probability of being at a node of the neutral network that has degree d is a constant times d . (Note that if d is the same for all nodes as in regular networks, we obtain the uniform distribution as expected.) Given the steady-state distribution, the histogram $P(h)$ of Hamming distances is determined from the fact that the lineages are independent. At large L , one expects it to become peaked, neutral networks being widely spread out in genotype space. Furthermore, the steady-state distribution and the $P(h)$ are M and μ independent.

Let us now allow for drift. The sampling of the parents takes place *with replacement*. Interestingly, the steady-state distribution of the population is not affected by the drift: this is due to the fact that the heterogeneity of the neutral network does not affect the chances of appearance of an offspring. However, the lineages are no longer independent since the population typically shares a recent common ancestor. As a consequence, the Hamming-distance distribution $P(h)$ is not determined from the steady-state distribution: it is non-trivial and depends on $M\mu$ at large M . Since this result holds in a far more general context which includes selection, we postpone its proof to the next section. *Corrections* to the $M\mu$ scaling are $O(1/M)$, with typically a rather small prefactor. In the $M\mu \rightarrow 0$ limit, just as in the general population dynamics [14], one recovers the blind ant dynamics.

For illustration, we show in Figures 2 and 3 the distribution of Hamming distances h for a population with myopic ant moves in the presence of drift on a neutral network. We see that in spite of the heterogeneity of the network, the $M\mu$ scaling holds just as for a homogeneous network.

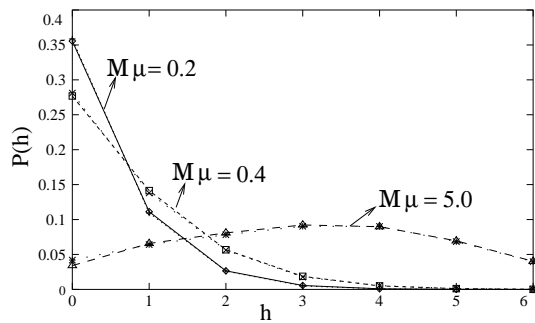


Figure 3. Distribution of Hamming distances h for different values of $M\mu$ for the myopic ant dynamics in the presence of drift. For each $M\mu$ we studied $M = 20$ and $M = 40$. The data with same $M\mu$ superimpose perfectly, exhibiting the $M\mu$ scaling.

6. Dynamics with selection and drift

6.1. The infinite-population (quasi-species) limit

In the infinite-population limit, $M \rightarrow \infty$ (with μ fixed), drift is absent and only the effects of mutation and selection show up; this is called the quasi-species regime [4, 5, 6]. As shown by van Nimwegen et al. [14], the steady-state distribution is given in this limit by the dominant eigenvector Ψ_0 of a linear operator defined by the adjacency matrix of the network. This eigenvector does not depend on μ , but its eigenvalue λ_0 does. If each individual in the population produced only one offspring, and the unviable ones were eliminated without replacement, then the population size would decay by a factor λ_0 at each generation. Relating this decay to the mutational robustness R_μ of the steady-state population we immediately obtain

$$\lambda_0 = (1 - \mu) + \mu R_\mu, \quad (2)$$

which yields the population's average neutrality $\langle d \rangle_\infty$ via equation (1): both R_μ and $\langle d \rangle_\infty$ are μ independent.

These results can be compared to the population neutrality in the case of blind/myopic ant moves, in which there is no explicit fitness-based removal of individuals. In the case of blind ants, the probability of residing on any node of the network is uniform. The average neutrality seen by such a walker is just equal to the average network neutrality. For a myopic ant, the probability of choosing any node on the network is proportional to the degree of the node. Neutrality is slightly higher in this case and is given by the ratio of second and first moments of the node degrees. A standard variational principle [29] shows that the population neutrality is always at least as large as the network neutrality, defined as the average degree of the neutral network. Of course on a homogenous graph, population neutrality, blind ant neutrality and myopic ant neutrality are all equal to the network neutrality. We refer the reader to the work of van Nimwegen et al. [14] for a thorough discussion.

6.2. Case of an infinite population at fixed $M\mu$

In biological situations, the mutation rate is very small, making the large- M limit of little use: indeed to get to the infinite M limit just discussed, the quantity $M\mu$ must be large. When $M\mu$ is finite, drift occurs, and it is of interest to consider the large M limit at fixed $M\mu$. In the *absence* of selection, the $M\mu$ scaling law has been derived by Derrida and Peliti [13]. In the presence of selection, it has been exhibited from numerical simulations by van Nimwegen et al. [14]. It turns out that this scaling follows from the dynamical equations, whether or not there is selection: these equations are invariant under a simultaneous rescaling of time, M and μ , as long as $M\mu$ is fixed, as we now show.

Let $N_i(g)$ denote the number of individuals in the population residing at the neutral network node i at generation g . To go to the next generation, let us choose M individuals at random with replacement, and let them mutate with probability μ . One then has

$$N_i(g+1) = \sum_{\langle ij \rangle} P_j(Mp_j) + G_i(Mq_i, Mq_i), \quad (3)$$

where $\sum_{\langle ij \rangle}$ denotes the sum over the nodes j which are nearest neighbors of node i . Also, $p_j = \mu N_i / (3LM)$ is the probability to choose an individual of genotype j and to have it mutate to node i ; $P_j(Mp_j)$ is a Poisson random variable of mean Mp_j ; $q_i = (1-\mu)N_i/M$ is the probability to choose an individual of genotype i and to leave it without mutation; $G_i(Mq_i, Mq_i)$ is the sum of M 0–1 random variables of mean q_i , and thus at large M is a Gaussian whose mean and variance are both given by Mq_i .

Since we are interested in the large M limit with $M\mu$ fixed, let us define $x_i = N_i/M$ to be the fraction of individuals residing on node i . If we average equation (3), we recover the deterministic (quasi-species) evolution equations for the x_i 's. But fluctuations do *not* go away at large M if $M\mu$ is fixed, instead the intensity of drift goes to a limit. Extracting the mean from the Gaussian of equation (3), the stochastic evolution equations for the x_i take the form

$$x_i(g+1) = (1-\mu)x_i(g) + \sum_{\langle ij \rangle} P_j(Mp_j)/M + G_i(0, Mq_i)/M. \quad (4)$$

Summing this expression over M steps we obtain in the limit of large M (and thus $\mu \rightarrow 0$):

$$\Delta x_i \equiv x_i(g+M) - x_i(g) = -M\mu x_i + \sum_{\langle ij \rangle} (M\mu)x_j/3L + G_i(0, x_i), \quad (5)$$

where we have used the fact that the sum of the M Poisson variables contributes via its mean but its variance (equal to p_j) becomes negligible. Clearly, the steady-state behavior of these stochastic equations depends only on the scaling parameter $M\mu$. As expected, by averaging these equations, we recover the quasi-species evolution dynamics. Strictly speaking, we have shown that there is a limit when evolving M individuals, neglecting the decrease in the population size. But restoring the population to a fixed size M involves no mutations and so falls into the standard case of drift for a single genotype; that stochastic process also reaches a limit at large M when $M\mu$ is fixed, so we can

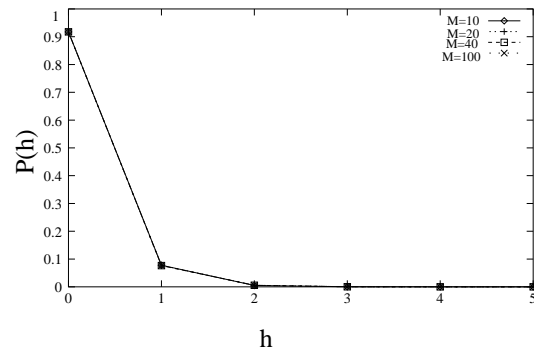


Figure 4. Distribution of Hamming distances at $M\mu = 0.2$ when $M = 10, 20, 40$ and 100 . The data superpose perfectly.

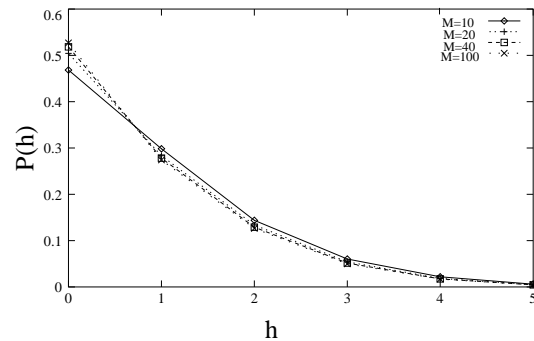


Figure 5. Distribution of Hamming distances at $M\mu = 2$ when $M = 10, 20, 40$ and 100 . The data collapse is excellent when $M \geq 20$.

conclude that the full process (which maintains the population size at M) also depends only on the scaling variable $M\mu$ as $M \rightarrow \infty$. Note that within this scaling framework, we recover the μ fixed, $M \rightarrow \infty$ case of equation (2) by taking $M\mu \rightarrow \infty$: we shall see that the corrections to this limit are linear in $1/M\mu$. One can also consider the limit $M\mu \rightarrow 0$: there, the population structure typically collapses to just one genotype at a time, and as shown by van Nimwegen et al. [14], the effective dynamics reduces to a random walk on the neutral network, so the population neutrality is given by the network neutrality.

6.3. Hamming distances in a finite population

We studied the distribution of Hamming distances between individuals in the steady state population evolving on our three RNA neutral networks. Here we report our results only for the largest network (of size 31484), as qualitatively similar results were obtained with the two other sizes.

If we fix $M\mu$, we obtain M -independent results when M is large, in agreement with the scaling law derived in the previous section. However, the value of M at which this scaling arises depends on $M\mu$. As shown in figures 4, 5, 6 and 7, the scaling sets in for

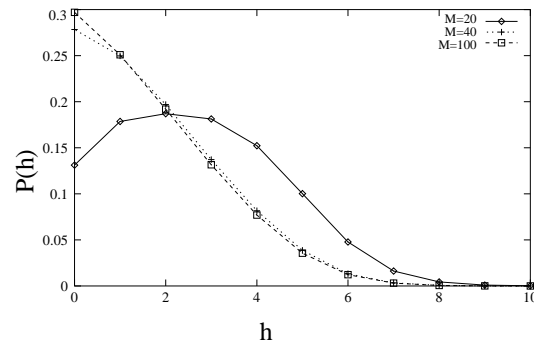


Figure 6. Distribution of Hamming distances at $M\mu = 5$ when $M = 20, 40$ and 100 . Here the data collapse requires $M \geq 40$.

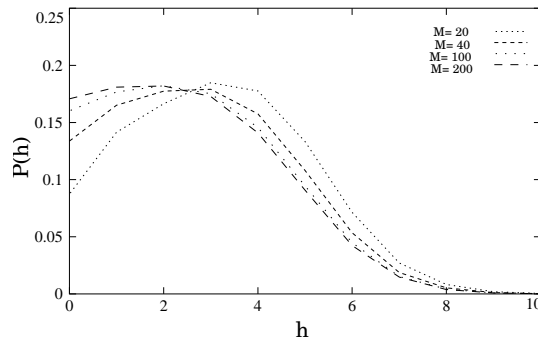


Figure 7. Distribution of Hamming distances at $M\mu = 10$ when $M = 20, 40, 100, 200$. The $M\mu$ scaling is good only for $M \geq 100$.

larger and larger values of M as the value of $M\mu$ grows. For instance, when $M\mu = 10$, one needs $M \geq 100$ to really see the $M\mu$ scaling convincingly (cf. figure 7). Moreover corrections to this scaling go as $O(1/M)$, i.e., they are of the same form as we found in section 5 in the absence of selection. This is a generic property that will be further studied in section 8.

Within the $M\mu$ scaling, we see the population spread increases monotonically with $M\mu$. In particular, as $M\mu \rightarrow 0$, the spread goes to 0, while as $M\mu \rightarrow \infty$, the population spreads across the whole neutral network.

6.4. Neutrality in a finite population

We first examine the population neutrality $\langle d \rangle_M$. We are interested in seeing how large M should be for the $M\mu$ scaling to set in, considering in particular the dependence on the neutral network size.

6.4.1. Small neutral network Figures 8(a) and (b) show the average neutrality $\langle d \rangle_M$ as a function of M and $M\mu$ respectively, for $\mu = 0.01, 0.1$ and 0.25 .

The average population neutrality depends both on M and $M\mu$. If μ is fixed and we

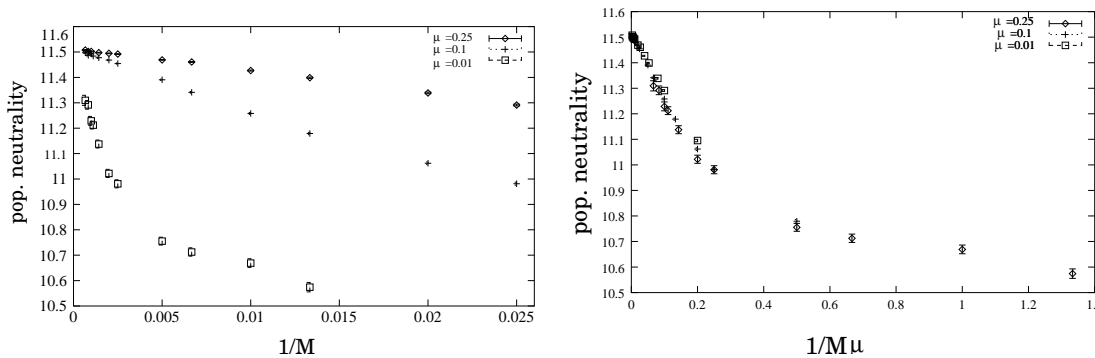


Figure 8. Population neutrality $\langle d \rangle_M$ as a function of $1/M$ and $1/M\mu$ for $\mu = 0.01, 0.1$ and 0.25 in our small size network. One can see the $M\mu$ scaling with small corrections due to finite M ; note also the linear behavior at the origin.

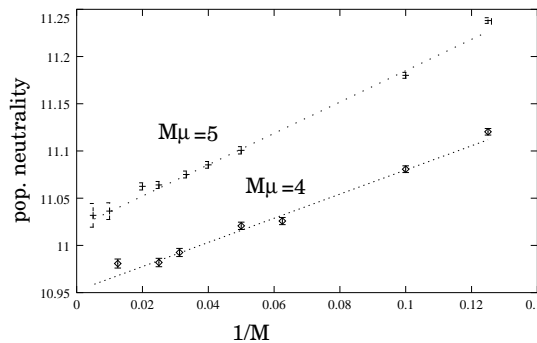


Figure 9. $1/M$ law for the corrections to $M\mu$ scaling.

take $M \rightarrow \infty$, we recover the quasi-species limit which is μ -independent. Similarly, for fixed $M\mu$, we obtain the $M\mu$ scaling regime by taking large M , just as in van Nimwegen et al. [14]. Furthermore, we see that the corrections to the large- $M\mu$ limit of population neutrality are linear in $1/(M\mu)$ (cf. the linear behavior at the origin in Figure 8(b)). Finally, the approach to the large M limit at fixed $M\mu$ has measurable $1/M$ corrections. (We also find that the value of $M\mu$ affects the time taken to approach the steady state.) At fixed $M\mu$, the dependence on M of the population neutrality or of the distribution of d is rather mild, though more marked than in the myopic or blind ant dynamics. For several values of $M\mu$, we show these $1/M$ corrections in figure 9. From all these data, we conclude that the population neutrality has the form

$$\langle d \rangle_M = f(M\mu) \left(1 + \frac{A(M\mu)}{M} + \dots \right), \quad (6)$$

where $f(M\mu) = \langle d \rangle_\infty$ is the $M \rightarrow \infty$ limit of $\langle d \rangle_M$ at given $M\mu$ and

$$f(M\mu) = f(\infty) \left(1 + \frac{B}{M\mu} + \dots \right), \quad (7)$$

describes how the large $M\mu$ limit converges to the quasi-species case. Finally, as shown by van Nimwegen et al. [14], $f(M\mu)$ tends to the network neutrality as $M\mu \rightarrow 0$.

6.4.2. *Medium and large networks* Similar results are found for our medium and large networks. Figure 10 shows the population neutrality as a function of $1/M\mu$, exhibiting good $M\mu$ scaling. However the corrections to this scaling are larger than those found in

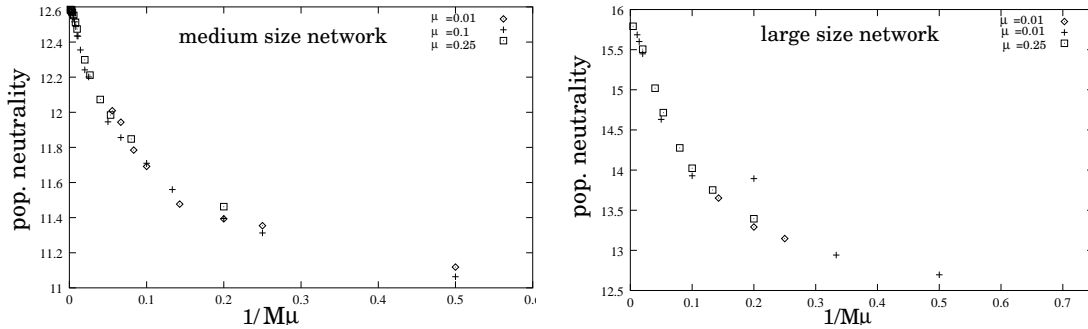


Figure 10. Average neutrality as a function of $1/M\mu$ for different values of μ on our medium and large size networks.

the small network; in fact, to see the asymptotic $1/M$ law for the corrections to the $M\mu$ scaling, one has to go to quite large values of M . Finally, as before, the quasi-species limit is reached with corrections $O(1/(M\mu))$.

Other results that seems to apply generally is that for fixed μ , the population neutrality (and thus the population robustness) increases with M , but it decreases at fixed $M\mu$. Mathematically, this means that $A > 0$ in equation (6) while $B < 0$ in equation (7).

7. Dynamics with selection but low drift

7.1. Framework

Random drift reduces the population spread and thus delays the approach to the large M limit at fixed μ . Lowering the drift would thus allow one to reach the large M limit more easily. Furthermore, one would have a higher mutational robustness of the steady-state population for a given population size; this higher survival probability suggests that biological mechanisms for reducing drift [30] could be selected for in natural populations. In this section we study dynamics in which selective pressures are high but the drift is particularly low.

Our dynamics on a neutral network is defined as follows so that drift effects are minimized:

- For a given population of size M and mutation probability per individual μ , we have $M\mu$ of the individuals in the population hop to any of their $3L$ neighbors; the others are unchanged. If a mutation brings an individual off the neutral network, we kill it, otherwise we keep it.
- We find the number of individuals that were killed and replace them by randomly cloning individuals from the remaining population.

Note that in these dynamics we perform a random sampling *only for a part of the population*; in fact, in the absence of selection, there is no drift at all.

To understand the essential difference from the usual dynamics, we use a branching process representation of the evolution and the cloning. An individual is represented by a point; at a given time there are M points for M individuals (note that as always M represents the number of individuals, not the number of different genotypes). From one generation (time) to the next, $M\mu$ points are replicated leading to branchings while the other points just proceed without branching. The time evolution generates branching processes in which each individual is represented by a point and is connected to its parent at the previous time by an edge. Following this branching process, we obtain the descendants of a given individual; one can also consider two individuals, follow their edges backwards till one reaches their most recent common ancestor. Because of the drift, at large enough times the whole population belongs to just one connected component.

Following Derrida and Peliti [13], let us investigate the genealogy of individuals going back in generations. For a subset of k individuals in the population, let $w_k(t)$ be the probability that their ancestors t generations ago were all different. To calculate this quantity, we first determine the probability x_k that k individuals have k distinct immediate ancestors (parents). Define $q = \mu(1 - \langle R_\mu \rangle_M)$ where $\langle R_\mu \rangle_M$ is the mean robustness of the population. Then assuming q is small and neglecting node to node fluctuations in neutrality, we have

$$x_k \approx 1 - \frac{k(k-1)q}{(1-q)M}. \quad (8)$$

Taking the generation-to-generation processes to be independent, one has $w_k(t) = x_k^t$, which can be approximated to leading order in q by

$$w_k(t) \approx \exp\left(-\frac{k(k-1)q}{M} t\right). \quad (9)$$

Hence, unlike the random drift case, the time scale is proportional to M/q . We thus define a rescaled dimensionless time variable

$$\tau = qt/M. \quad (10)$$

The probability that the two individuals shared a common ancestor at most t generations back is given by $1 - w_2(t) = 1 - \exp(-2\tau)$. Thus the probability density $p(\tau)$ that the most recent common ancestor of the two individuals arose between $\tau M/q$ and $(\tau + d\tau)M/q$ generations ago is given by

$$p(\tau) = \frac{d(1 - w_2(\tau))}{d\tau} = 2\exp(-2\tau). \quad (11)$$

Therefore the characteristic time for the most recent common ancestor scales as M/μ , while it scales as M in the usual dynamics with drift of section 6.

The distribution of times to the most recent common ancestor can be used to obtain the Hamming-distance distribution of the steady-state population. Let $\phi_\nu(t)$

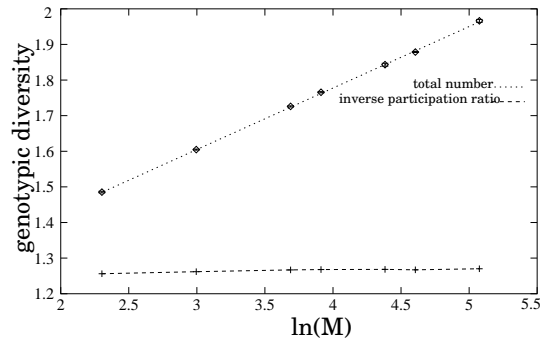


Figure 11. Plot of genotypic diversity (g_M and G_M) for dynamics with selection and drift as function of $\ln M$ at $M\mu = 0.4$.

be the probability that two random walkers in genotype space find themselves at a Hamming distance ν given that they coincided t generations before. We have

$$\phi_\nu(t) = \frac{\Gamma[L+1]}{2^\nu \Gamma[\nu+1] \Gamma[L-\nu+1]} (1 - \exp^{-2\mu t})^\nu, \quad (12)$$

where L is the genome length. Then P_ν , the probability that the Hamming distance between two individuals in the steady state population is equal to ν , is given by

$$P_\nu = \int_0^\infty d\tau p(\tau) \phi_\nu(t). \quad (13)$$

Using the expression of $\phi_\nu(t)$ from equation (12), one sees that P_ν depends on M but not much on μ ; in particular, one has a well defined $\mu \rightarrow 0$ limit at fixed M . This is to be contrasted with the random drift case where P_ν depends mainly on $M\mu$.

7.2. Consequence for the genotypic diversity

A high level of genotypic diversity in a population is usually advantageous for survival. Here we study how low drift can greatly enhance this diversity by examining two measures of the number of different genotypes, namely the actual number g_M (which is frequency independent), and the inverse participation ratio G_M of the genotypic abundances. Explicitly, for a population of size M , if the number of individuals with genotype i is m_i , we define

$$G_M = \frac{(\sum m_i)^2}{\sum m_i^2}, \quad (14)$$

where the sum runs over all the different genotypes present in the population.

We show in figure 11 the two different measures of genotypic diversity for dynamics with selection and drift. The bottom curve corresponds to G_M , the top one to g_M . We find that the “absolute” genotypic diversity g_M , (taking into account genotypes of arbitrarily low frequencies), grows logarithmically (and thus rather slowly) with M at fixed $M\mu$. On the other hand, the rare genotypes contribute less to the inverse participation ratio G_M , and we find that this measure of genotypic diversity saturates in the large M limit at fixed $M\mu$.

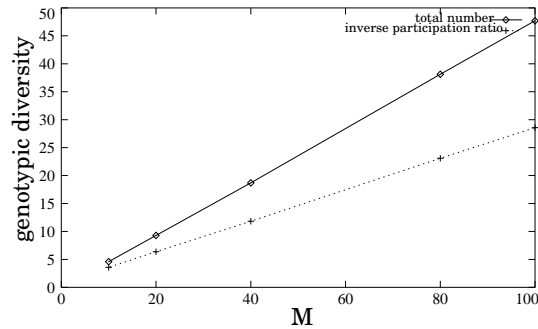


Figure 12. Plot of genotypic diversity (g_M and G_M) as a function of population size M for dynamics with selection but low drift at $M\mu = 0.4$.

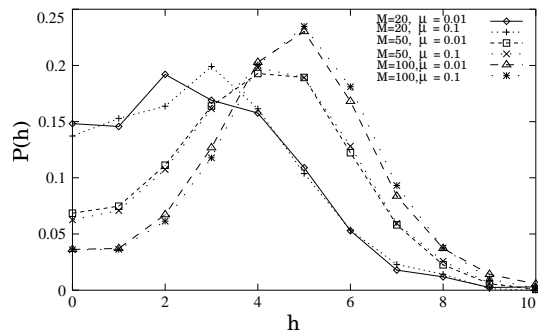


Figure 13. Distribution of Hamming distances for evolutionary dynamics with low drift. The distributions depend strongly on M and only very weakly on μ .

In Fig. 12 we display the same quantities for our low-drift dynamics. We now see that both measures of diversity grow linearly with M at fixed $M\mu$; thus each genotype in the population arises just a few times as $M \rightarrow \infty$ if $M\mu$ is fixed. Clearly the reduction of drift in this dynamics allows for a high genotypic diversity.

7.3. Hamming distances

We can study Hamming distances as was done in section 6.3 for our low-drift dynamics. We find that the distribution of Hamming distances depends strongly on M but not much on μ and approaches a μ -independent limit as M grows large (figures 13 and 14). This is consistent with the above calculation for the scaling laws. As expected, for fixed M , there is a non-trivial limit distribution as $\mu \rightarrow 0$.

7.4. Population neutrality

In the infinite population limit, the value of population neutrality is independent of drift effects, and it is also independent of μ . Consider first our small neutral network with 489 nodes and network neutrality 10.4499; we determined the largest eigenvalue of the adjacency matrix (via *Mathematica* [31]), obtaining $\langle d \rangle_\infty = 11.5107$. In a finite

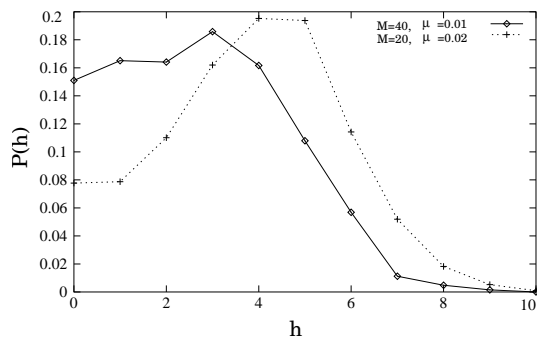


Figure 14. Distribution of Hamming distances for two different values of population size (20 and 40) when $M\mu=0.4$, showing the absence of $M\mu$ scaling when the dynamics has low drift.

population we find that $\langle d \rangle_M$ approaches $\langle d \rangle_\infty$, with $1/M$ corrections that do not depend much on the mutation rate. In particular, we find

$$\langle d \rangle_M = \langle d \rangle_\infty \left(1 + \frac{A(\mu)}{M} \right), \quad (15)$$

where $A = -0.328 \pm 0.002$ for $\mu = 0.1$ and $A = -0.317 \pm 0.005$ for $\mu = 0.25$. The corresponding fits are shown in figure 15.

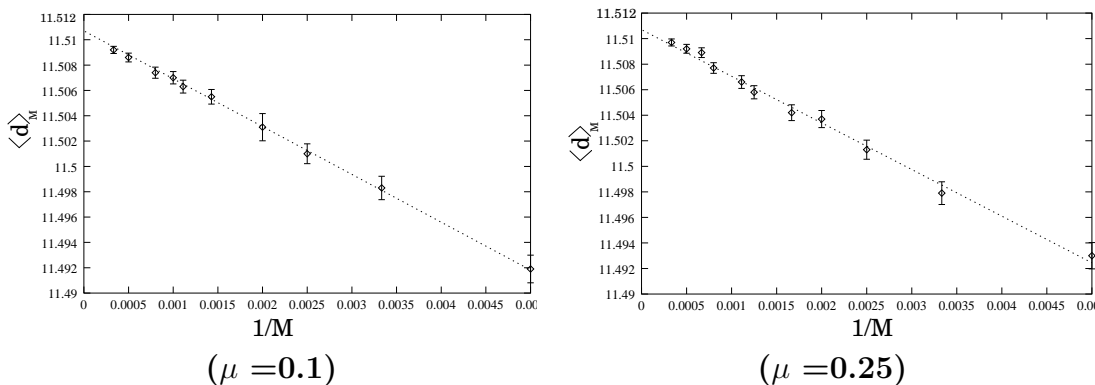


Figure 15. Population neutrality vs $1/M$ on the small size network. The dotted line is a linear fit as in Eq. (15).

On our medium-size neutral network (with 5784 nodes), we find that the network average neutrality is equal to 10.6888, while $\langle d \rangle_\infty = 12.592 \pm 0.0002$. We again find a $1/M$ convergence as in Eq. (15) with $A = -0.752 \pm 0.035$ for $\mu = 0.05$ and $A = -0.662 \pm 0.02$ for $\mu = 0.25$ (figure 16). Just as for the small neutral network, A does not depend much on μ .

Finally, on the large neutral network (with 31484 nodes), we find the network neutrality to be 12.116, whereas $\langle d \rangle_\infty = 15.434$. Figure 17 confirms the $1/M$ convergence with $A = -0.927 \pm 0.045$ for $\mu = 0.05$ and $A = -0.944 \pm 0.044$ for $\mu = 0.25$.

The overall pattern is thus that the data are well represented by equation (15), with an $A(\mu)$ that grows with increasing network size and depends slowly on μ . We have

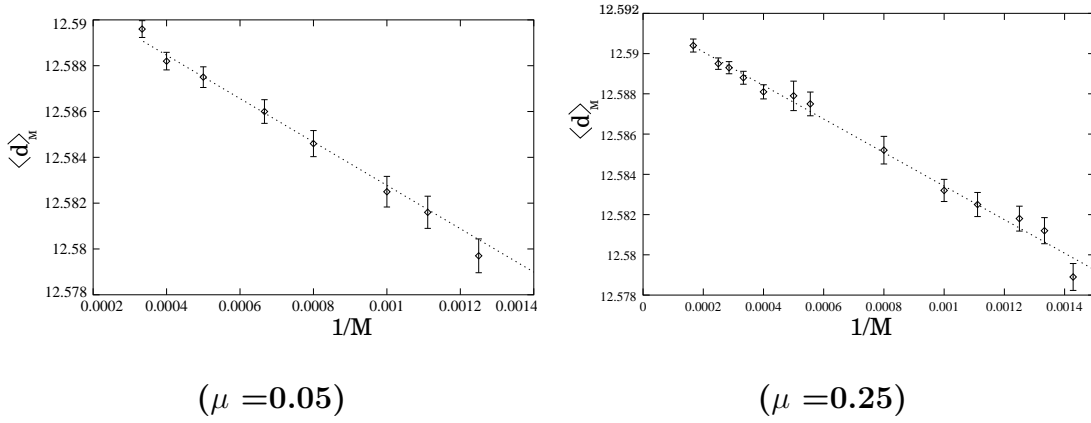


Figure 16. Population neutrality vs $1/M$ on the medium size network. The dotted line is a linear fit as in Eq. (15).

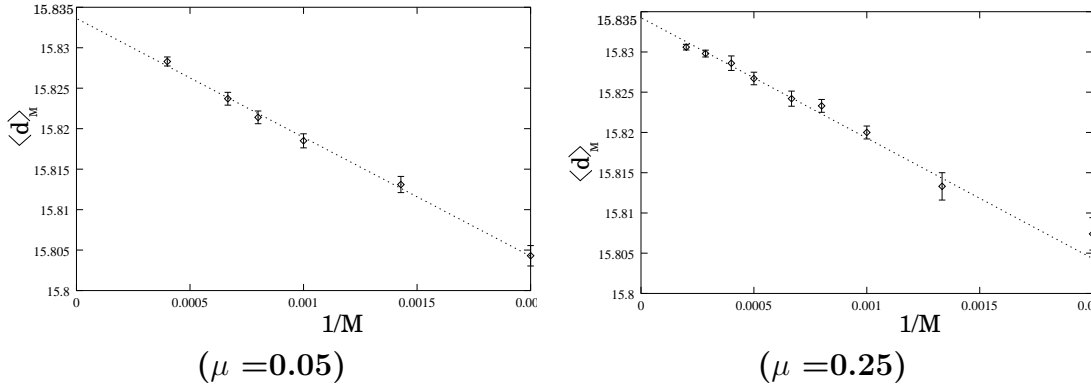


Figure 17. Population neutrality vs $1/M$ on the large size network. The dotted line is a linear fit as in Eq. (15).

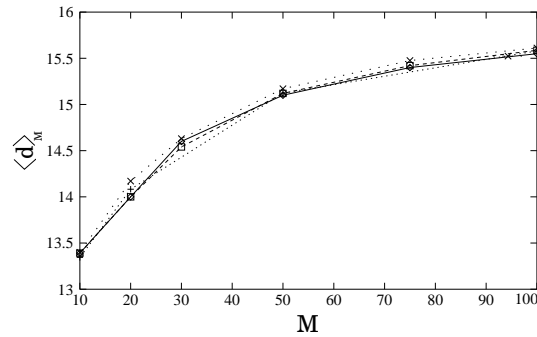


Figure 18. Population neutrality $\langle d \rangle_M$ vs M for $\mu = 0.01, 0.05, 0.1$ and 0.25 on the large neutral network, showing the insensitivity to μ .

also checked directly that $\langle d \rangle_M$ is rather insensitive to the value of μ (cf. figure 18). Furthermore, in all cases, there is no $M\mu$ scaling (cf. figure 19), in contrast with what happens for the case of standard drift (see section 6).

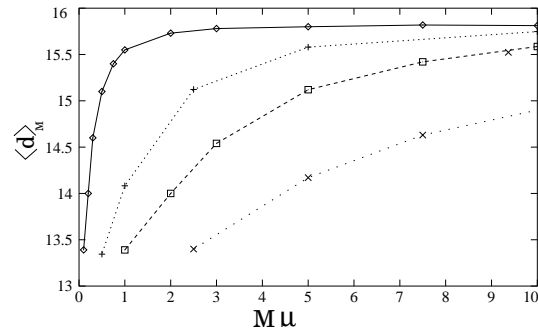


Figure 19. Population neutrality $\langle d \rangle_M$ vs $M\mu$ for $\mu = 0.01, 0.05, 0.1$ and 0.25 on the large neutral network, showing the absence of $M\mu$ scaling.

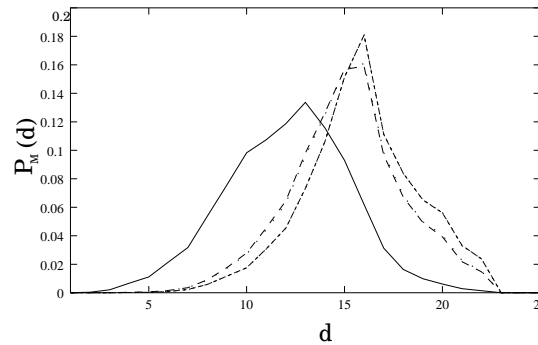


Figure 20. The continuous line shows the distribution of the number of neighbors for random nodes on the largest network (with 31484 nodes). The curve closest to it shows the steady state distribution for two data sets, with $\mu = 0.1$ and 0.25 when the population size is 50: they superpose extremely well. The third curve corresponds to $M = 1000$ and $\mu = 0.1, 0.25$ and 0.5 , again with excellent superposition. Superposition (independence on μ) becomes exact when $M = \infty$.

7.5. Distribution of neutrality

As a last point, let us consider the whole distribution $P_M(d)$ rather than just the average population neutrality $\langle d \rangle_M$. In figure 20 we display several cases of interest for our largest neutral network. The left-most curve is for genotypes chosen randomly and uniformly from the neutral network. The next curve on the right is for a population of size $M = 50$ undergoing selection with low drift; there are in fact two data sets displayed, one for $\mu = 0.1$ and one for $\mu = 0.25$. The last curve is for the same algorithm at $M = 1000$ for three values of μ , namely $\mu = 0.1, 0.25$ and 0.5 .

Several comments are in order. First, as M increases, the overall trend is for $P_M(d)$ to shift to larger d ; this is in agreement with the general property that mutational robustness grows with increasing genotypic diversity. Second, there is hardly any dependence of these data on μ , a feature particular to dynamics having reduced drift.

8. Reaching the large M limit and barriers in the fitness landscape

8.1. Motivation

For large populations in the presence of drift, the relevant parameter appears to be $M\mu$, as we have seen in sections 5 and 6. When one wishes to evaluate the large- M limit at given μ , it is better to minimize drift as in section 7, especially when μ is small, since μ plays little role in this modified dynamics. We also saw that the corrections to the $M = \infty$ limit go like $O(1/M)$ on neutral networks. Simple arguments [32] suggest that this is a generic property of growth with diffusion phenomena, and we shall now confirm this on toy landscapes: the $O(1/M)$ corrections are not an artefact of the fitness being 0 and 1 as we have assumed so far. Furthermore, we wish to get some insight into the *size* of this correction. For our three neutral networks, we found that the factor A of the A/M correction grows with increasing neutral network size; however, barriers (entropic or fitness) in the landscape are likely to affect A , as we will now illustrate using a few toy landscapes.

8.2. Evolution in a toy fitness landscape

To build up our intuition, we will consider a space where genotypes are parametrized by a real number, and mutations correspond to small changes of this number. Evolution in low-dimensional fitness landscapes has been considered by several authors in the recent years and has led to a number of insights (see, e.g., [33, 34, 35, 36]). In this case, it is convenient to consider a continuous-time limit because this allows for a Fokker-Planck formulation. We can start with all individuals at the same position or place them randomly in the landscape. After some time, the population reaches a well defined steady state. For the numerical simulation of such evolutionary dynamics, we discretize time using a time step Δt ; this then gives the following update rules:

- At each step (small) mutations arise; this means that the genotype x is changed by Δx where Δx is a Gaussian random variable of standard deviation $\sqrt{2D\Delta t}$ [37].
- Given the new positions of the individuals, we allow for replication according to fitness given by a function $-V(x)$ in the Fokker-Planck language. $V(x)$ is low (or even negative) if the genotype has a high fitness; it is large and positive for an unfit genotype. Then for an interval Δt of time, an individual of genotype x will be killed with probability $1 - \exp(-V(x)\Delta t)$ if $V(x) > 0$; if instead $V(x) < 0$, a clonal birth will be produced with probability $\exp(-V(x)\Delta t) - 1$. Following standard practice, if one wants to keep the population size fixed on average near some target value M , one simply shifts additively $V(x)$ so that the expected population size is precisely M .

In the $M \rightarrow \infty$ limit, the details associated with keeping the population at its target value no longer matter and the overall process can be formulated as a rate equation. Up

to the rescaling of the population to keep its size fixed, the density of genotypes $\rho(x)$ follows the deterministic equation

$$\frac{\partial \rho(x, t)}{\partial t} = D \frac{\partial^2 \rho(x, t)}{\partial x^2} - V(x) \rho(x, t). \quad (16)$$

This is a linear evolution law that is the continuum analog of the quasi-species dynamics. At large times the *shape* of $\rho(x)$ converges to the eigenfunction of the linear operator on the right hand side whose eigenvalue is largest. One can recognize (16) as being an (imaginary time) Schrödinger equation. The problem of the steady-state distribution is thus mathematically a simple one that can be solved analytically for particular choices of the function $V(x)$. Now we can address the question of *how* the large M limit is reached.

8.3. Harmonic well

We first consider the case where $V(x) = x^2$, which corresponds in the Schrödinger equation framework to diffusion in a harmonic well, a case with no barriers. In the $M \rightarrow \infty$ limit, the probability distribution of the population in this landscape is $P(x) = \exp(-x^2/2)/\sqrt{2\pi}$.

For a finite population of size M , we evaluate numerically the steady state distribution $P_M(x)$. We see a clear convergence of this distribution to its large- M limit, with $1/M$ corrections:

$$P_M(x) = P(x) \left(1 + \frac{K(x)}{M} \right) + O(M^{-2}). \quad (17)$$

The $1/M$ nature of the convergence clearly appears in figure 21, where we see that the amplitude of these corrections is small. This kind of convergence has been justified before [32] in the context of population algorithms for solving linear evolution operators. Furthermore, it is possible to show that the correction function $K(x)$ goes to a constant at large x . When we obtain such a data collapse, we know M is large enough for one to extract $P(x)$.

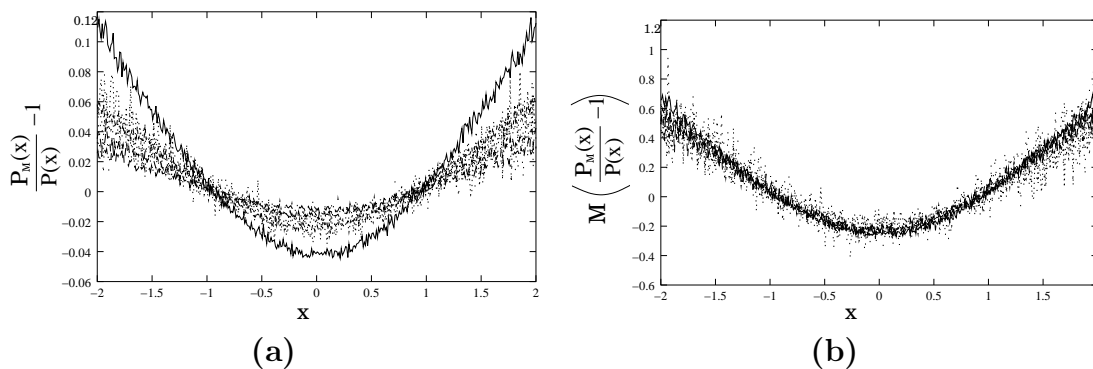


Figure 21. (a) Relative deviation $P_M(x)/P(x) - 1$ vs x for $M = 6, 8, 10, 12, 15$ and 20 . (b) Data collapse plot: $M(P_M(x)/P(x) - 1)$ for $M = 6, 8, 10, 12, 15$ and 20 .

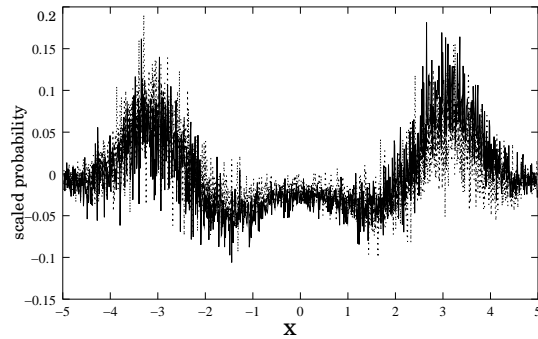


Figure 22. Data collapse plot for $M_1 M_2 (P_{M_1}(x) - P_{M_2}(x)) / (M_1 - M_2)$ vs x , for several population sizes M_1 and M_2 , in the case of a symmetric double well. We have taken $(M_1, M_2) = (6, 10), (10, 20), (6, 20), (20, 50)$

8.4. Symmetric double well

We now consider the case of a landscape with two degenerate optima separated by a barrier (passage of low fitness). For that we take $V(x)$ to be an even polynomial of degree 4 in x : $V(x) = V(-x)$. Since $P(x)$ is not analytically known, we examine instead the quantity $M_1 M_2 (P_{M_1}(x) - P_{M_2}(x)) / (M_1 - M_2)$ for different population sizes M_1 and M_2 . If the convergence goes as $O(1/M)$, then, provided M_1 and M_2 are sufficiently large, the data should collapse onto a limit function. This is indeed what we find; the case $V(x) = x^2 + 0.1x^4$ is used for illustration in figure 22.

8.5. Case of an asymmetric double well

To go from one fitness peak to another, one has to cross a barrier. The previous double well has a symmetric steady state, and even with a small population, this symmetry is realized. However when the well is asymmetric, finite population effects will be quite larger. Indeed, in the $M \rightarrow \infty$ limit, even a small non symmetric part ($V(x)$ not even in x) will lead to a distribution practically concentrated in one well. (This is called the “flea and elephant phenomenon” well known in quantum mechanics: when the barrier between the two wells is high, even a tiny difference in V between the two sides leads to a big effect, just as when a little itching on an elephant’s shoulder leads it to put all of its weight onto one side.) When the population is finite, this effect is not so evident, and the two wells remain nearly symmetrically populated. One has to go to large population sizes M in order to come closer to the $M \rightarrow \infty$ limit.

To investigate this effect quantitatively, we consider the asymmetric potential $V(x) = -x^2 + bx^4 + cx$ with $b = 0.05$ and $c = 0.002$, corresponding to an asymmetry of roughly 0.1%. We found the $1/M$ convergence law, but had to go to $M \approx 100$ to observe the data collapse. This is shown in figure 23; note the large scale of the y axis compared to the symmetric double well case: the $1/M$ corrections are much larger here. When the barrier height is increased, one needs even larger M values to see the $M = \infty$ limit: the proper balance of population on each side of the barrier sets in very slowly in M .

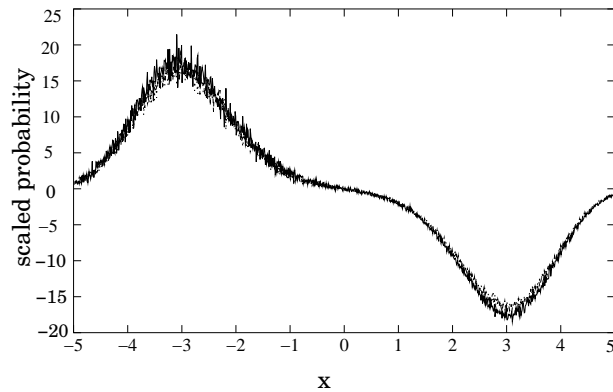


Figure 23. Data collapse plot for $M_1 M_2 (P_{M_1}(x) - P_{M_2}(x)) / (M_1 - M_2)$ vs x , for several population sizes M_1 and M_2 , in the case of an asymmetric well. $M = 200, 250, 300, 400, 500$.

In landscapes with more than one dimension, there can also be entropic barriers, that is passages that are narrow but not of particularly low fitness; such cases are relevant for general neutral networks.

9. Summary and conclusions

In general, an evolving population undergoes mutation, selection and random drift. In this work we quantified the effect of these processes to untangle the different effects, using neutral networks and toy fitness landscapes for illustration. In the case of infinite populations, there have been many studies. If $M\mu \rightarrow \infty$, (M being the population size and μ the mutation rate), drift is absent and one recovers the quasi-species limit [4, 5, 6], with results that developed by van Nimwegen et al. [14] in the context of neutral networks. For finite $M\mu$ ($M \rightarrow \infty$), drift effects are important; there, in the absence of selection, Derrida and Peliti [13] derived a number of important results. In this work we have considered the case $M\mu$ finite with selection, for both M finite and infinite. We derived the $M\mu$ scaling even in the presence of selection. The (finite M) *corrections* to this $M\mu$ scaling are $O(1/M)$, be there selection or not. When $M = \infty$, we find that the quasi-species limit is reached via $1/M\mu$ corrections. In all cases, $M\mu$ plays the role of an effective population size. These laws are summarized in equations (6) and (7). We also found that the amplitude of the correction terms showed a slow increase with neutral network size. In practice, the $M\mu$ scaling sets in at relatively small values of M . Furthermore, at fixed $M\mu$ we showed that the genotypic diversity g_M of the population increases only logarithmically as a function of M .

Finally, we considered a dynamics with low drift in section 7. Drift is effectively reduced by a factor μ and thus genotypic diversity always grows *linearly* with population size even if $M\mu$ is fixed. One thereby avoids the $M\mu$ scaling law, a useful property if one wishes to evaluate the large- M limit at small μ . Nevertheless, reaching this limit can be seriously hindered by fitness or entropic barriers in the fitness landscape as we

saw in section 8.

Acknowledgments

This work was supported by the EEC's FP6 IST Programme under contract IST-001935, EVERGROW. We thank F. Hospital and A. Wagner for their comments. LP is grateful to the LPTMS for its hospitality when this work was started.

References

- [1] Herron J C and Freeman S R 2003 *Evolutionary Analysis* (Prentice Hall)
- [2] Wright S 1932 *Proc. of the Sixth Int. Congress on Genetics* vol 1 ed Jones D F (Austin, TX) pp 356–366
- [3] Gavrilets S 2004 *Fitness Landscapes and the Origin of Species* (Princeton: Princeton University Press)
- [4] Eigen M 1971 *Naturwissenschaften* **58** 465
- [5] Eigen M and Schuster P 1977 *Naturwissenschaften* **64** 541
- [6] Eigen M, McCaskill J S and Schuster P 1989 *Adv. Chem. Phys.* **75** 149–263
- [7] Stadler P F 2002 *Biological Evolution and Statistical Physics* ed Lässig M and Valleriani A (Berlin: Springer) pp 183–204
- [8] Schuster P 2002 *Biological Evolution and Statistical Physics* ed Lässig M and Valleriani A (Berlin: Springer) pp 56–83
- [9] Lieberman E, Hauert C and Nowak M 2005 *Nature* **433** 312–316
- [10] Taylor C, Fudenberg D, Sasaki A and Nowak M 2004 *Bull. Math. Biol.* **66** 1621–1644
- [11] Roca C P, Cuesta J A and Sanchez A 2006 *Phys. Rev. Lett.* **97** 158701
- [12] Antal T, Redner S and Sood V 2006 *Phys. Rev. Lett.* **96** 188104
- [13] Derrida B and Peliti L 1991 *Bull. Math. Biol.* **53** 355–382
- [14] van Nimwegen E, Crutchfield J P and Huynen M 1999 *Proc. Natl. Acad. Sci. USA* **96** 9716–9720
- [15] Ewens W 2004 *Mathematical Population Genetics - I. Theoretical Introduction* (New York: Springer Verlag)
- [16] Fontana W, Stadler P F, Bornberg-Bauer E G, Griesmacher T, Hofacker I L, Tacker M, Tarazona P, Weinberger E D and Schuster P 1993 *Phys. Rev. E* **47** 2083–2099
- [17] Lipman D J and Wilbur W J 1991 *Proceedings: Biological Sciences* **245** 7–11
- [18] Grüner W, Giegerich U, Strothmann D, Reidys C, Weber J, Hofacker I, Stadler P and Schuster P 1996 *Monath. Chem.* **127** 375–389
- [19] Kauffman S and Levin S 1987 *J. Theor. Biol.* **128** 11–45
- [20] Flyvbjerg H and Lautrup B 1992 *Phys. Rev. A* **46** 6714–6723
- [21] van Nimwegen E and Crutchfield J P 2000 *Bull. Math. Biol.* **62** 799–848
- [22] Reidys C, Schuster P and Stadler P 1997 *Bull. Math. Biol.* **59** 339–397
- [23] Fontana W and Schuster P 1998 *J. Theor. Biol.* **194** 491–515
- [24] Schuster P and Stadler P 2002 *Complexity* **8** 34–42
- [25] The Vienna package 1995 <http://www.tbi.univie.ac.at/~ivo/RNA/>
- [26] Huynen M A, Stadler P F and Fontana W 1996 *Proc. Natl. Acad. Sci. USA* **93** 397–401
- [27] Hughes B D 1996 *Random Walks and Random Environments* (Oxford: Clarendon)
- [28] Orr H A 2003 *J. Theor. Biol.* **220** 241–247
- [29] Soshnikov A and Sudakov B 2003 *Comm. Math. Phys.* **239** 53–63
- [30] Whitlock M, Ingvarsson P and Hatfield T 2000 *Heredity* **84** 452
- [31] Mathematica 2005 Wolfram Research, <http://www.wolfram.com>
- [32] Cerf N J and Martin O C 1995 *Int. J. of Modern Physics C* **6** 693–723
- [33] Tsimring L S, Levine H and Kessler D A 1996 *Phys. Rev. Lett.* **76** 4440–4443

- [34] Kessler D A, Levine H Ridgway D and Tsimring L 1997 *J. Stat. Mech.* **87** 519–544
- [35] Peng W Q, Gerland U, Hwa T and Levine H 2003 *Phys. Rev. Lett.* **90** 088103
- [36] Rouzine I M, Wakeley J and Coffin J M 2003 *Proc. Natl. Acad. Sci. USA* **100** 587–592
- [37] van Kampen N G 1981 *Stochastic Processes in Physics and Chemistry* (Amsterdam: North-Holland)